Journal of Materials Chemistry B

PAPER

View Article Online
View Journal | View Issue

Cite this: J. Mater. Chem. B, 2018, 6, 940

Polydopamine–polyethylene glycol–albumin antifouling coatings on multiple substrates†

S. C. Goh,[a] Y. Luan,[b] X. Wang,[b] H. Du,[b] C. Chau,[a] H. E. Schellhorn,[c] J. L. Brash,*[a] H. Chen[b] and Q. Fang*[ad]

Received 2nd October 2017,
Accepted 15th January 2018

DOI: 10.1039/c7tb02636f

rsc.li/materials-b

Aqueous-based coatings using combinations of polydopamine (PDA) (as bioadhesive) and grafted polyethylene glycol (PEG) (as antifouling agent) have been reported to reduce biofouling on multiple material surfaces. However, the achievable PEG grafting density and antifouling performance are limited, leaving exposed PDA to provide sites for attachment of proteins and cells. In the present work, we investigate the polymerization of dopamine on three substrate materials, polycarbonate membrane (PC), polydimethyl siloxane (PDMS), and soda lime glass, to evaluate the utility of the PDA coatings for application to multiple materials. Additionally, we propose that the PDA–PEG method may be improved by "backfilling" with bovine serum albumin (BSA) as a blocker covering exposed PDA. AFM and ellipsometry studies revealed substantial differences in PDA thickness and roughness on each material despite their being modified under the same conditions. X-ray photoelectron spectroscopy (XPS) and water contact angle data revealed differences in PEG grafting on these materials as a consequence of varying PDA surface roughness, with the highest PEG coverage achieved on PC–PDA surfaces of intermediate roughness and lower PEG attachment on smoother PDMS–PDA surfaces. Fibrinogen adsorption experiments showed significantly less fouling on PDA–BSA surfaces compared to PDA–PEG for all three substrates, the larger BSA molecules presumably providing greater coverage of the PDA. On the PC and PDMS substrates, backfilling the PDA–PEG surfaces with BSA gave significant reductions in fibrinogen adsorption, with the lowest adsorption of 75 ng cm^{-2} achieved on PC–PDA–PEG/BSA.

Introduction

Preventing unwanted protein adsorption on devices used in biomedicine and biotechnology is important to improve biocompatibility, control cell adhesion, and reduce biofouling. Surface modification is preferred to create long-lasting, non-toxic coatings on biomaterials by changing the surface chemistry for desired applications. In water quality monitoring, sensor devices are expected to operate without intervention or maintenance in harsh environments.[1,2] Antifouling surface modifications allow these water sensors to operate remotely in fixed locations, providing real-time continuous monitoring of water quality.[1,3] Antifouling surface modifications have also been used to control protein adsorption and cell adhesion in multi-functional microfluidic assays,[4] blood contacting materials,[5] and for biosensing applications.[6]

In the past few years, new sensing and imaging devices constructed with multiple materials, *e.g.* polycarbonate (PC), polydimethyl siloxane (PDMS), glass, and silicon, have been developed.[7,8] These emerging devices require surface modification methods that are compatible with their fabrication and operation. Modification of each material using different methods is potentially costly since processes, equipment, and reagents may vary. Furthermore, an assembled device cannot be modified 'differentially' (*i.e.* using a different process in different areas) due to the possible damage of surfaces by later-stage processing. Therefore, a single antifouling method suitable for multiple materials and whole device modification is highly desirable.[9,10]

Surface modification by grafting hydrophilic polymers is widely used to create highly protein- and cell-resistant surfaces. The protein resistance of grafted hydrophilic polymers is dependent on the grafting density, chain length and chain configuration on the surface.[11] Polymer brushes, *i.e.* structures in which the polymer chains are extended, are structures of high chain density and, in the case of hydrophilic polymers such as polyethylene glycol (PEG), high water content.[5,11,12] Hydrophilic polymer brushes constitute an "osmotic barrier"

[a] School of Biomedical Engineering, McMaster University, Hamilton, ON, Canada. E-mail: qiyin.fang@mcmaster.ca, brashjl@mcmaster.ca
[b] College of Chemistry, Chemical Engineering and Materials Science, Soochow University, Suzhou, Jiangsu, P. R. China
[c] Department of Biology, McMaster University, Hamilton, ON, Canada
[d] Department of Engineering Physics, McMaster University, Hamilton, ON, Canada

† Electronic supplementary information (ESI) available: AFM–water and AFM–air comparison. See DOI: 10.1039/c7tb02636f

that effectively leads to a loss of entropy as protein molecules approach, thereby inhibiting adsorption.[6,11,13] Highly protein resistant surfaces (adsorption below 20 ng cm^{-2}) have been created using grafting-from techniques such as atom-transfer radical polymerization (ATRP), reversible addition–fragmentation chain-transfer (RAFT) polymerization, nitroxide mediated polymerization (NMP), and iniferter-based polymerization.[9,14] However, these techniques generally involve the use of harsh solvents, harsh reaction conditions, and laborious procedures. The utility of such a surface modification strategy is then dependent on the substrate's initial surface chemistry and tolerance to these harsh conditions. Thus, these protocols are in general designed for and limited to a specific material.

For biological applications, aqueous-based methods avoiding organic solvents and harsh reaction conditions, and with applicability to a wide range of materials are highly desirable.[9,10] Dopamine is a water soluble compound that has attracted much interest as an adhesive for the surface modification of biomaterials.[15] Oxidized dopamine monomers can strongly self assemble from solution to form polydopamine (PDA) layers on virtually all types of materials, including polymers, metals, and composites.[13,15,16] PDA is reported to be highly stable in aqueous environments, strong acids, and mild redox environments for extended periods of time.[15,17] PDA coatings are favourable for surface modification because they are not only versatile and non-toxic, but can react readily with a wide range of amino- and thiol-containing biomolecules.[16] Recently, PDA and catechol derivatives have been studied to attach species such as polysaccharides,[18] peptides,[19] and zwitterions,[20] to surfaces.

Aqueous-based antifouling coatings using water soluble, preformed hydrophilic polymers grafted to PDA films (*i.e.* grafting-to method) have been widely reported following the pioneering research of Lee *et al.*[10] Antifouling PDA–PEG coated surfaces have been used on filtration membranes for food protein analysis,[17,21] water filtration membranes,[22,23] bioassays and cell patterning,[24,25] and antibacterial surfaces.[26] However, due to the high reactivity of PDA with amino groups, PDA coated surfaces are strongly protein adsorbing.[16,27,28] Since PEG grafting onto PDA is conducted using pre-formed PEG chains, the packing density is limited, and areas of PDA not covered by PEG are available to adsorb proteins.[13,29] Pop-Georgievski *et al.*[13] reported a low polyethylene oxide (PEO) grafting density (0.16 nm^{-2}) and correspondingly low protein resistance on gold–PDA surfaces. Miller *et al.*[23] reported a decrease in resistance to bacterial adhesion of PDA–PEG coated polysulfone ultrafiltration membranes after three to four days in a biofouling environment.

It is reasonable to expect that PDA–PEG antifouling surfaces can be improved by ''backfilling'' with bovine serum albumin (BSA). ''Backfilling'' is intended to block protein adsorption to exposed PDA. BSA is essentially bioinert and has been used to reduce non-specific protein adsorption in solid phase immunoassays,[30–32] and mammalian[33–36] and bacterial cell adhesion.[37,38] It has been proposed that BSA inhibits the adhesion of negatively charged bacteria due to electrostatic and steric repulsion, low surface interaction energy, or BSA folding to an inactive conformation upon adsorption.[37,38] Furthermore, saturated BSA monolayers have been shown to inhibit the adsorption of cell adhesive proteins[35,37,39] which may contribute to the inhibition of cell adhesion. BSA can be covalently attached to PDA through its free amino groups (*e.g.* on lysine residues).[27,30] The formation of stable covalent bonds between BSA and the PDA should prevent protein exchange between BSA and other proteins in a contacting medium.

In the present work, PDA–PEG antifouling coatings on three substrate materials, polycarbonate membrane (PC), polydimethyl siloxane (PDMS), and soda lime glass, were investigated to evaluate the utility of PDA-based coatings for application to multiple materials. In addition, the anti-fouling behaviour of the PDA–PEG coatings backfilled with BSA was examined.

Experimental

Chemicals and materials

Sylgard® 184 silicone elastomer kit was purchased from Dow Corning (Midland, MI) to prepare the PDMS surfaces. Hydrophilic polycarbonate track etch membranes with 0.01 μm pore size were purchased from Sterlitech Corporation (Kent, WA). This material is pre-coated with polyvinylpyrrolidone (PVP) by the manufacturer to make the surface hydrophilic and improve its compatibility in aqueous environments. Square soda lime glass cover slips (5 × 5 mm) were purchased from Haimen Aibende Experiment Equipment Co. Ltd (Nantong, P. R. China). Amino–PEG–amine (MW 5000 Da) was purchased from Jenkem Technology USA Inc. (Plano, TX). Dopamine hydrochloride and BSA (>98%, lyophilized powder) were purchased from Sigma-Aldrich (Oakville, ON, Canada). Human fibrinogen was purchased from Enzyme Research Laboratories (South Bend, IN). AG® 1-X4 Resin was purchased from Bio-Rad (Mississauga, ON). Sodium iodide-125 ($Na^{125}I$) isotope purchased from the McMaster Nuclear Reactor (McMaster University, Hamilton, ON) was used to label fibrinogen. Organic solvents of analytical grade were used as received. 10× Phosphate buffered saline (PBS) from BioShop Canada Inc. (Burlington, ON) at pH 7.4 was reduced to 1× strength using Milli-Q water (18.2 MΩ cm) from Millipore Co. The pH of PBS was raised to 8.5 using sodium hydroxide (NaOH).

Substrate preparation

Polydimethyl siloxane (PDMS) approximately 1 mm thick was prepared using a Sylgard® 184 silicone elastomer kit. The base and curing agent were mixed in a 10 : 1 ratio by weight and cured at 60 °C for 4 h. The film was then punched into 6 mm diameter discs. Circular polycarbonate membranes (PC) of 25 mm diameter were divided and cut into 8 triangular pieces each of area 1.23 cm^2. Glass samples were used as received. All substrates were rinsed with 95% ethanol and Milli-Q water before surface modification.

PDA modification

PC, PDMS, and glass samples with dimensions as previously noted were immersed in a 2 mg mL^{-1} dopamine solution

freshly prepared from dopamine hydrochloride in PBS adjusted to pH 8.5 with NaOH. The samples were shaken in an open glass dish at room temperature for 3 h. The newly modified surfaces were thoroughly rinsed with Milli-Q water. All dopamine-coated surfaces were stored in fresh Milli-Q water to prevent transfer of the polydopamine modification onto the storage container. PDA is stable in water and water protects the PDA layer from cracking or transferring onto its contacting surface during the drying process.[40]

PDA post-modification by PEG and BSA

PDA coated surfaces were shaken for 24 h at 37 °C in 5 mg mL^{-1} PEG (PBS, pH 8.5). PDA–PEG surfaces were then backfilled with BSA by incubation with shaking in 10 mg mL^{-1} BSA solution (PBS, pH 7.4) for 24 h at 21 °C. The protocol is shown schematically in Fig. 1. PDA–BSA surfaces backfilled with PEG were prepared in the conditions previously described but in reverse order. Surfaces were thoroughly rinsed and stored in Milli-Q water after modification in each solution.

Atomic force microscopy (AFM)

AFM height images of PDA modified surfaces were taken using a Veeco Dimension Icon AFM (Plainview, NY). The AFM images were obtained in air under ambient conditions using ScanAsyt mode with PeakForce tapping. The silicon nitride cantilever (spring constant $k = 0.4$ N m^{-1}) was automatically adjusted to a scan rate of 1 Hz and set to acquire 512 samples per line. NanoScope Analysis software ver.1.5 by Bruker Corporation was used for image analysis. PDA particle analysis was conducted on features above the surface. Threshold height values were set to incorporate the maximum number of PDA particles for analysis. Surface roughness was reported as the average root mean square (R_{rms}) roughness taken over the entire image. The roughness parameter was defined as the root mean square average of the height deviations taken from the mean data plane as described by eqn (1),

$$R_{rms} = \sqrt{\frac{1}{N}\sum_{i=1}^{N}(h - \bar{h})} \quad (1)$$

where $\bar{h}$ is the mean data plane height, h is the current height value, and N is the number of points within the selected image region.[41] AFM data are reported as mean ± SD for three 2 × 2 μm images.

Ellipsometry

Polydopamine layer thickness was determined using a variable angle spectroscopic ellipsometer (J. A. Woollam Co., Lincoln, NE). PDMS was cured on 1 mm thick glass slides and modified with PDA as described. PC–PDA samples were placed on silicon wafers to improve the optical contrast of the sample pores. Glass slides were modified with PDA as described. Measurements were performed over a wavelength range of λ = 245–1700 nm at angles of incidence 55, 60, 65, and 70° for PDMS and glass. For PC, measurements were performed over a wavelength range λ = 1000–1700 nm since complete depolarization of the incident light occurred below 1000 nm. PC measurements were conducted at angles of incidence 70° and 75°, which provided the greatest signal intensity. Ellipsometry data were modelled using CompleteEASE software v.4.65 developed by J. A. Woollam Co. The Cauchy model was used as the base for glass. PDMS and PC base were modelled using the B-Spline layer. Due to the porous nature of PC, anisotropic B-Spline was applied with refractive index n_{PC} = 1.625 and 1.58 as specified by the manufacturer. The PDA layer was modelled using the Cauchy model with refractive index set to n = 1.45.[40,42] The absorption coefficient was determined as k = 0.01399. A graded model was used for the PDA layer on glass with an average inhomogeneity of −41.8 ± 11.9%. The average thickness and roughness of PDA were reported for n = 3 measurements with modelling confidence specified by $MSE_{PC} < 6$, $MSE_{PDMS} < 2$, and $MSE_{glass} < 8$.

X-ray photoelectron spectroscopy (XPS)

XPS spectra were recorded using a Physical Electronics (PHI) Quantera II spectrometer. X-rays were generated with an aluminium anode source and focussed with a quartz crystal monochromator. The monochromatized aluminium Kα X-ray source at 1486.7 eV was operated at 50 W and 15 kV. A dual beam charge compensation system was used for neutralization. Survey spectra were obtained with 280 eV pass energy at a 45° take off angle. Elemental compositions of the surfaces were determined from low resolution scans for C, O, N and Si. Data treatment was performed using PHI MultiPak Version 9.4.0.7 software. One measurement per sample type was carried out at two surface locations (spot size 200 μm).

Water contact angles

Samples were air dried before measurement. Water drops of 6 μL were placed on the surface and advancing contact angles were measured after 2 min using a goniometer (Krüss DSA100, Hamburg, Germany) at room temperature. Contact angles for n = 3 samples per modification were recorded.

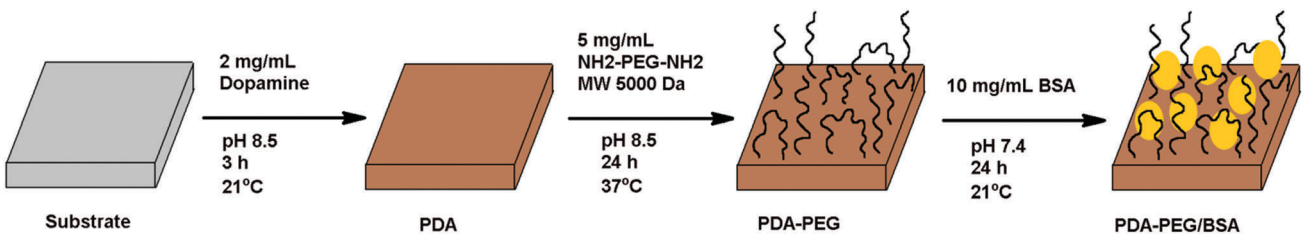

Fig. 1 Protocol for surface modification of PC, PDMS, and glass. PEG attachment may be through one or both NH_2 chain ends giving stretched or looped chains, respectively.

Radiolabeled fibrinogen adsorption

Fibrinogen was radiolabeled with $Na^{125}I$ using the iodine monochloride method.[43] The radioactive fibrinogen solution was passed through a column of AG 1 × 4 anion exchange resin to remove unbound iodide ion. Tests were conducted to determine residual free iodide. Briefly, labelled protein was precipitated in trichloroacetic acid (TCA) and centrifuged. The supernatant, containing free iodide ion (*i.e.* not bound to protein) was counted on a Wizard Automatic Gamma Counter (Perkin Elmer, Boston, MA). Levels below 1% were deemed acceptable.

The surfaces were incubated in fibrinogen solutions containing 5% I-125-labelled fibrinogen and diluted in PBS to a final concentration of 1 mg mL^{-1}. After 2 h incubation at room temperature, the surfaces were rinsed three times in PBS (pH 7.4). Surface radioactivity was determined by γ-counting. The mass density of protein on the surface was calculated by comparing the surface radioactivity to that of a solution of labelled fibrinogen of known concentration. The experiments were repeated three times using three different batches of samples modified independently.

E. coli adhesion

PDMS surfaces were sterilized in 70% EtOH and rinsed with Milli-Q water prior to cell seeding. *E. coli* K12 stably transfected with GFP from plasmid was inoculated from agar into LB media supplemented with 25 μg mL^{-1} Kanamycin antibiotics. The culture was allowed to grow until an optical density of 0.4 was reached; it was then centrifuged and the pellet re-suspended in PBS (pH 7.4). PDMS samples modified with PDA–PEG/BSA were scratched with tweezers to reveal bare PDMS. The substrates were then incubated in 1 mL of medium containing 2×10^7 cells per mL for 4 h in a rotary shaker (200 rpm, 37 °C). The samples were gently rinsed three times (5 min each time) with PBS before imaging with an epifluorescence microscope (Evos FL Auto, Life Technologies, USA) equipped with a YFP LED light cube (ex. 500/24 nm; em. 524/27 nm) at 20× objective. Images were enhanced with ImageJ v1.45s analysis software.

Statistical analysis

Student's *t*-tests were conducted on all data sets with significance level set at p-value < 0.05.

Results and discussion

PDA layer formation: thickness and surface roughness

Minimizing the surface roughness of PDA layers is recommended to facilitate post-modification.[13] Over time, the polymeric/polymerizing dopamine in solution begins to aggregate forming colloidal particles of increasing size.[13,40] These particles spontaneously adsorb to the substrate material, generating an uneven surface. High surface roughness caused by the adsorption of large PDA particles may hinder coverage subsequently of the PDA by PEG or other modifiers. The optimal PDA thickness to achieve a hole-free layer while maintaining minimal surface roughness is suggested to be 10–20 nm, obtained typically after 2–4 h incubation at room temperature.[13] Thus, a PDA incubation time of 3 h was chosen for this study. After 3 h dopamine polymerization the PC, PDMS, and glass surfaces acquired a distinctive brown tinge characteristic of PDA as shown in Fig. 2.[15]

Data on thickness and surface roughness of the PDA layers as determined by ellipsometry and AFM are summarized in Table 1. AFM scans used to determine surface roughness and particle features are shown in Fig. 2. A roughness value for PC could not be determined by ellipsometry due to near complete depolarization and low intensity of the reflected light at $\lambda < 1000$ nm. Surface roughness is modelled at shorter wavelengths due to higher scattering of light at these wavelengths.[44] Since strong depolarization was observed on unmodified PC, light depolarization was limited to the PC substrate and did not include the PDA deposit. It is suspected that strong anisotropic light scattering leading to light depolarization was most likely the cause. This effect is due to the birefringent nature of the porous PC membrane (n_{PC} = 1.625 and 1.58). To accurately model the PDA thickness on PC, wavelengths below 1000 nm were eliminated from the analysis. PDA thickness on PC was determined to be 6.3 ± 0.1 nm. PDA roughness was determined to be 16.5 ± 4.4 nm from AFM analysis. "Divots" in the PDA surface caused by the pores of the membrane were observed in AFM scans, although the extent of pore coverage by PDA was uncertain.

The thickness of PDA on PDMS was determined to be 27 ± 5 nm by ellipsometry. Larger area AFM scans of PDMS–PDA shown in Fig. 3(a) revealed cracks in the PDA layer, likely formed during sample drying. The PDA thickness on PDMS from the AFM scan, as shown in Fig. 3(b), was reported to be 25.5 nm and is within the PDA thickness range determined by ellipsometry. This provided strong evidence that the material at the lowest point of the cracks was likely bare PDMS or PDMS minimally covered by PDA. PDA cracking was observed only for PDMS, possibly due to the flexibility of this material. The surface roughness of PDMS also increased after PDA deposition, with a feature size of about 7 nm as determined by both AFM and ellipsometry.

Ellipsometry measurements on glass–PDA samples showed the PDA thickness to be 11 ± 3 nm. Despite the fact that glass was the smoothest of the three unmodified substrates, glass–PDA showed the highest roughness after modification: 36.8 ± 1.4 nm by AFM; 50 ± 13 nm by ellipsometry. Although the ellipsometry value appears higher than the AFM, the values are not significantly different (p-value = 0.051).

PDA particle analysis

Variability in PDA thickness and roughness on the three materials revealed substantial differences in dopamine polymerization on these substrates. From the AFM scans shown in Fig. 2, it is clear that the PDA particles formed on each material were of very different morphologies. Since colloidal PDA particles have been reported to increase in diameter over time,[13] particle analysis was performed as a means of probing differences in dopamine polymerization on the three materials.

PDMS–PDA showed the lowest surface density and largest diameter of PDA grains. However, the PDA thickness on PDMS

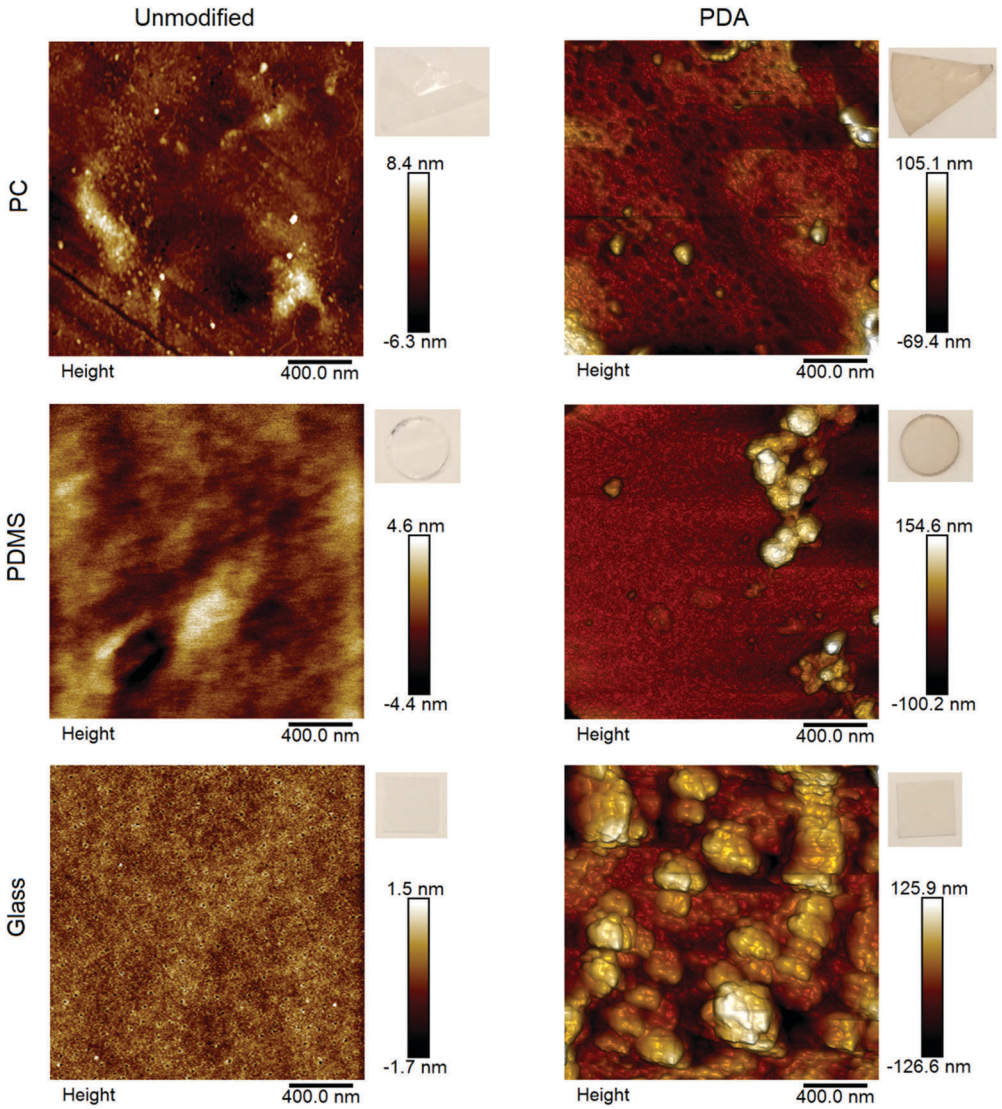

Fig. 2 AFM topographic images and photographs of unmodified and PDA-modified PC, PDMS, and glass samples. Samples were tinted with a distinctive brown colour after 3 h dopamine polymerization at room temperature and samples remained brown after subsequent modifications with PEG and BSA.

Table 1 Surface characteristics of PDA deposited on PC, PDMS, and glass as determined by ellipsometry and AFM. The average root mean square (R_{rms}) surface roughness parameter and grain characteristics are reported for three 2 × 2 μm AFM scans. AFM scans are shown in Fig. 2. Data are means ± SD, n = 3

	PDA thickness (nm)	Roughness (nm)				
Surface	Ellipsometry	Ellipsometry	AFM (R_{rms})	Density of grains (μm^{-2})	Average grain height (nm)	Average grain diameter (nm)
PC	—	N/A	3.0 ± 1.3	—	—	—
PC–PDA	6.3 ± 0.1	N/A	16.5 ± 4.4	22 ± 6	17 ± 7	69 ± 25
PDMS	—	0 ± 0	1.3 ± 0.1	—	—	—
PDMS–PDA	27 ± 5	7 ± 1	9.8 ± 2.8	1.3 ± 0.4	46.5 ± 8.4	273 ± 21
Glass	—	1.1 ± 0.02	0.8 ± 0.3	—	—	—
Glass–PDA	11 ± 3	50 ± 13	36.8 ± 1.4	7 ± 3	52 ± 1	129 ± 29

was found to be greater than on PC or glass. This suggests that PDA deposition on PDMS may occur primarily by direct polymerization on the surface rather than adsorption/deposition of colloidal particles formed in solution, leading to a greater density of PDA (and hence, a thicker PDA layer) while minimizing PDA surface roughness. The affinity of dopamine for the hydrophobic PDMS thus appears to be high, causing rapid and extensive adsorption and polymerization.

The AFM images of PC and glass surfaces showed a greater variety of PDA particle structures. The greater surface roughness values for PC and glass compared to PDMS appear to be due to stacking of PDA particles as they adsorbed on the surface.

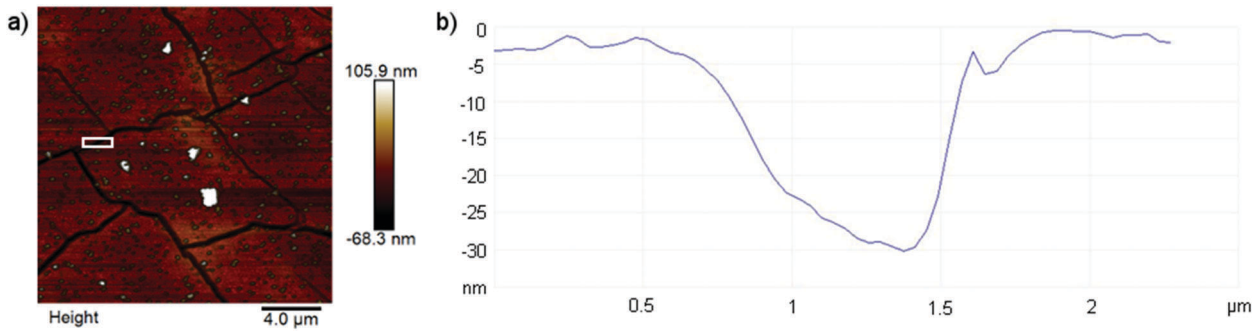

Fig. 3 (a) Large area (20 × 20 µm) AFM height image of PDMS–PDA revealing cracks in the PDA layer. (b) Vertical distance map across the white boxed area in (a). PDA thickness = 25.5 nm.

PC–PDA showed the highest grain density with the smallest grain size, indicating that PDA particle deposition on PC was favoured early in the process. However, glass–PDA showed almost twice the average grain diameter and one-third the average grain density compared to PC–PDA. These larger PDA grains on glass surfaces are attributed to glass–PDA showing the highest surface roughness of the three materials.

Since all three materials were modified under the same reaction conditions, PDA particle growth in the solution should be the same. It appears that the attractive forces between dopamine/PDA and the substrate may influence whether dopamine polymerizes directly on the substrate or if polydopamine–melanin particles formed in solution deposit on the surface. Since the surfaces bear no formal charge, the affinity of dopamine may be determined mainly by surface wettability. PDA interactions with the hydrophilic glass may be relatively weak and require larger PDA particles (formed in solution) for adhesion to occur. PDA interactions with PC, of intermediate wettability, may be moderate allowing smaller particles to adsorb to the surface early. Shearing at the PC–PDA surface due to stirring of the solution may explain why the particle size did not increase. Interactions of dopamine with hydrophobic PDMS may be strong promoting adsorption and polymerization on the surface. Since the starting surface roughness values of the three materials were similar (AFM roughness: PC = 3.0 ± 1.3, PDMS = 1.3 ± 0.1, and glass = 0.8 ± 0.3 nm), it is not possible to know from our results whether initial surface roughness affects early dopamine polymerization.

It should be noted that the AFM images in Fig. 2 and 3 were obtained in air. However the materials are intended for use in aqueous contact. To check whether the surfaces in air and water showed major structural differences, a few images were obtained in contact with water. The surfaces appeared essentially the same in both media (p-value > 0.05 for surface roughness and particle features) as typified by the wet and dry images of PDA-modified glass shown in Fig. S1, ESI.†

The major conclusion from this analysis of PDA deposits is that although PDA layers were formed on all three substrates, the properties of the layers were by no means identical, and indeed showed major differences. Substrate wettability may have affected dopamine polymerization and adsorption of dopamine–melanin particles at the surface, thus forming different PDA layers on the three materials. It is expected that these differences will be reflected in the interactions of cells and proteins with the PDA deposits.

XPS analysis

The elemental compositions of bare and modified PC, PDMS, and glass surfaces as determined by XPS are presented in Table 2. On all three surfaces the nitrogen level increased significantly upon deposition of PDA. It should be noted that the high N content on the starting PC surface is due to the PVP coating on this material. Due to the presence of carbon in the unmodified substrates, the carbon data cannot be used to determine whether the N and C contents after PDA modification are consistent with theoretical predictions for PDA. Eqn (2), adapted from Michel *et al.*,[45] can be used to obtain the true signal of an element, X, by correction for an over-layer using a substrate specific signal as a reference. In the present case, Si can be used as the substrate specific element for PDMS and glass:

$$X_{\text{true}} = X_{\text{f}} - X_{\text{i}}\left(\frac{\text{Si}_{\text{f}}}{\text{Si}_{\text{i}}}\right) \quad (2)$$

where X_{True} is the corrected element signal, X_{f} and Si_{f} are the post-modification signals, and X_{i} and Si_{i} are the pre-modification signals.

Using the corrected values for C, the nitrogen-to-carbon ratio (N/C) was determined to be 0.094 for PDMS and 0.121 for glass. These values are close to the theoretical N/C ratio of 0.125 for PDA.[10] In addition, the Si content of PDMS and glass decreased upon PDA deposition due to masking of the substrate. Incomplete masking of the Si signal on glass is in line with a thickness value of 11 ± 3 nm for the PDA layer as measured by ellipsometry, *i.e.* lower than the sampling depth of XPS (~10 nm). On PDMS, the PDA thickness determined by ellipsometry was greater than the XPS sampling depth, so the Si detected was most likely due to gaps in the PDA layer exposing bare PDMS as was seen in AFM images (Fig. 3).

Due to the lack of a substrate specific element for PC, the true C and N signals contributed by PDA could not be calculated. However, the large increase in N content after PDA modification and the change in substrate colour (Fig. 2) provided evidence that PDA was indeed deposited on the surface. The uncorrected N/C ratio for PC–PDA was 0.086 and the PDA thickness was

Table 2 XPS elemental composition (percent) of PC, PDMS, and glass surfaces modified with PDA, PEG and BSA

Surface	C 1s	N 1s	O 1s	Si 2p
PC	79.9	2.6	17.5	0.0
PC–PDA	67.8	5.8	24.0	2.5
PC–PDA–PEG	69.4	7.3	21.4	1.3
PC–PDA–BSA	68.0	10.8	20.1	1.1
PC–PDA–BSA/PEG	69.9	10.0	19.1	1.1
PC–PDA–PEG/BSA	70.1	8.4	20.0	0.8
PDMS	44.2	0	31.1	24.7
PDMS–PDA	49.8	1.3	28.8	20.1
PDMS–PDA–PEG	51.6	1.4	29.0	18.0
PDMS–PDA–BSA	54.0	3.7	27.0	15.3
PDMS–PDA–BSA/PEG	51.4	3.0	28.7	16.9
PDMS–PDA–PEG/BSA	51.9	3.2	27.8	17.1
Glass	12.7	0	61.4	22.8
Glass–PDA	54.2	6.0	31.0	8.0
Glass–PDA–PEG	45.7	5.0	37.2	11.3
Glass–PDA–BSA	35.4	6.2	42.6	14.7
Glass–PDA–BSA/PEG	20.0	1.0	56.0	22.7
Glass–PDA–PEG/BSA	28.1	3.7	48.8	18.6

Estimated XPS data precision ± 0.5%

6.3 ± 0.1 nm, suggesting that substrate-specific carbon was being detected.

On PC–PDA surfaces, a further increase in N content was observed after the attachment of amino-terminated PEG and BSA. The increase was greater for BSA as expected due to the higher N content contributed by lysine residues. PC modified with PDA–BSA and PDA–BSA/PEG showed similar elemental compositions. Attachment of PEG to PDA–BSA was likely difficult due to covering of most of the available binding sites on PDA by the large BSA molecule. However, when PEG preceded BSA (PDA–PEG–BSA surface), the N content was intermediate between those of PDA–PEG and PDA–BSA, suggesting that both PEG and BSA were present.

On glass–PDA it appears that the PDA layer suffered damage on exposure to BSA and PEG so changes in nitrogen content may not simply reflect the attachment of these molecules. The increase in Si and decrease in N content after PEG and BSA treatments suggest that PDA was removed during these steps. The Si content was restored almost to that of the unmodified glass after PEG/BSA and BSA/PEG treatments. Mechanical removal of PDA may have occurred *via* contact with other samples or container walls during treatment. No loss of PDA was observed on PDMS–PDA and PC–PDA after further treatment, although PDMS was also found to be prone to mechanical damage during sample handling.

Water contact angles

Water contact angle data are shown in Table 3. Angles on PDA-modified surfaces have been reported to be in the range 50° to 65° independent of substrate after 24 h incubation with dopamine.[15,40,46] Under these conditions PDA layers of thickness greater than 10 nm are typically formed.[10] As seen in Table 3, the contact angle on PDMS decreased from 117° to 67° after 3 h incubation in dopamine solution, while that on glass increased from 16° to 41°. The angles on PDMS–PDA and glass–PDA were thus in the vicinity of those for PDA surfaces previously reported. The angle on PC decreased slightly from 66° to 58°, again within the range previously reported.

Table 3 Water contact angles on unmodified and modified PC, PDMS, and glass. Angles using 6 μl water droplets were measured after 2 min of surface contact. Mean ± SD, n = 3

Modification	PC	PDMS	Glass
Unmodified	66° ± 2°	117° ± 3°	16° ± 2°
PDA	58° ± 7°	67° ± 8°	41° ± 4°
PDA–PEG	38° ± 2°	54° ± 3°	24° ± 2°
PDA–BSA	65° ± 4°	72° ± 2°	54° ± 1°
PDA–BSA/PEG	33° ± 1°	72° ± 7°	38° ± 3°
PDA–PEG/BSA	34° ± 2°	60° ± 5°	36° ± 2°

The wide range in contact angles after various PEG and BSA modifications among the three materials in the present study may be due to the differences in PDA coverage. Nevertheless, for all three substrates the water contact angles were reduced on treatment of the PDA surfaces with PEG. PDMS–PDA surfaces showed the smallest decrease, supporting XPS data indicating inefficient PEG attachment, but the fact that there was a decrease suggests that some PEG was attached. PDA surfaces modified with BSA showed higher contact angles than those modified with PEG. These results are consistent with the findings of Zhu *et al.*[27] who reported decreased hydrophilicity of PDA–BSA coated PE membranes (θ_i = 61.6) compared to PDA coated PE membranes (θ_i = 46.7).

The combination of BSA and PEG resulted in varying contact angles dependent on the degree of attachment of the first compound. The high wettability of PDA–BSA/PEG and PDA–PEG/BSA on PC suggests that the PEG coverage was greater than the BSA. Poor PEG attachment on PDMS–PDA resulted in the wettability of PDA–BSA/PEG and PDA–PEG/BSA to be more similar to a BSA surface. Surface damage (as seen in XPS data) may have contributed to the low contact angle for glass–PDA modified with BSA/PEG and PEG/BSA. Thus, PEG and BSA coverage could not be directly interpreted from the contact angle data for glass surfaces.

Fibrinogen adsorption

Fibrinogen adsorption data are presented in Fig. 4. In agreement with previous observations,[16,27] adsorption was high on all PDA-modified materials, presumably due to reaction between the catechol/quinone groups in PDA and the amino/thiol groups in the protein. Adsorption on all surfaces was reduced upon attachment of PEG; the reduction was significantly greater on PC–PDA (56%) than on PDMS–PDA (40%). The lower effective surface area on PDMS presumably reduced the availability of reactive PDA sites for PEG attachment, resulting in a lower PEG density. The reduction in adsorption on glass–PDA–PEG *vs.* glass–PDA was still lower (35%). However, PEG grafting efficiency based on inhibition of fibrinogen adsorption should not be compared between glass and the other substrates since the PDA layer on glass was probably damaged, as indicated by the XPS data.

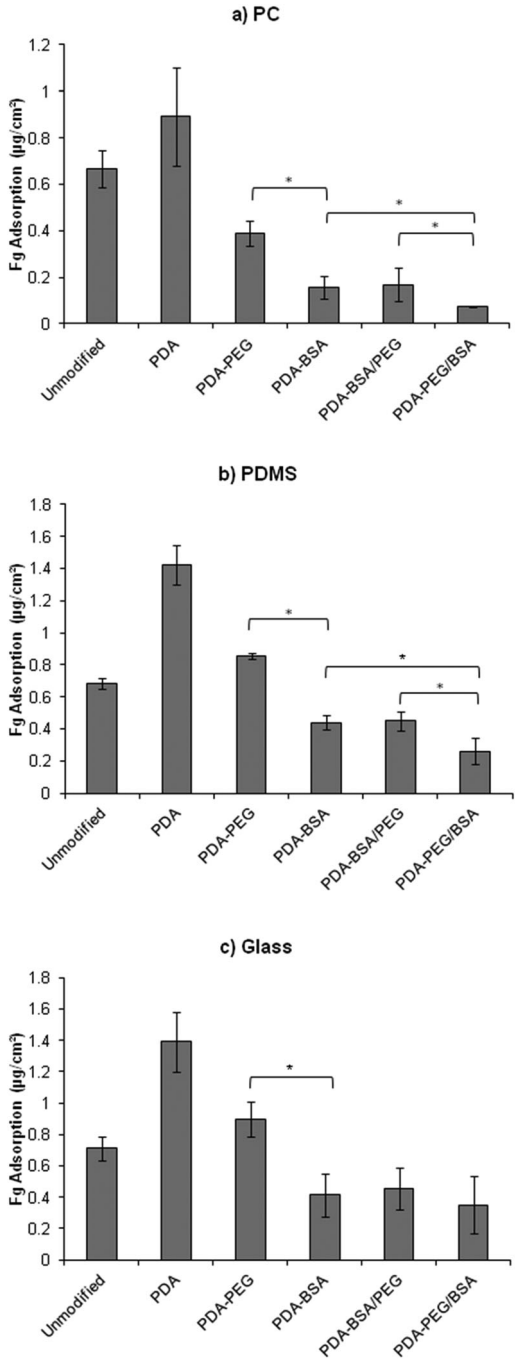

Fig. 4 Fibrinogen adsorption on unmodified and modified surfaces: (a) PC, (b) PDMS, (c) glass. Fibrinogen 1 mg mL^{-1} in PBS pH 7.4. Adsorption time, 2 h at 21 °C. Data are mean ± SD, n = 3. * Difference significant at p-value < 0.05.

Attachment of BSA directly to the PDA surfaces reduced fibrinogen adsorption to a significantly greater extent than attachment of PEG for all three substrates (82 *vs.* 56% for PC; 69 *vs.* 40% for PDMS; 70 *vs.* 35% for glass) presumably due to the more effective masking of PDA by the large BSA molecules and the well-known strong blocking effect of BSA. Furthermore, backfilling of the PDA–BSA surfaces with PEG had no effect on fibrinogen adsorption. It is likely that most of the PDA attachment sites were occupied by BSA and little PEG was attached to these surfaces. On the other hand, backfilling of the PDA–PEG surfaces with BSA reduced adsorption significantly on all three substrates, indicating that significant gaps were present on the PDA–PEG surfaces allowing attachment of BSA. This again confirms the strong affinity of PDA for proteins and that BSA has strong blocking power for fibrinogen. For all substrates, differences in fibrinogen adsorption among the three modifications involving BSA were small (in some cases not significant), suggesting that all of these surfaces consisted predominantly of BSA. However, the PDA–PEG–BSA surfaces were the most fibrinogen resistant, indicating more complete masking of PDA or synergy of some kind between BSA and PEG in that case. The PC–PDA–PEG/BSA surface was the most resistant of all the surfaces investigated with an adsorption level of 75 ng cm^{-2}.

These fibrinogen adsorption data provoke the following observations concerning PDA-modification as a basis for preparing protein-resistant, antifouling surfaces on multiple substrates. In the antifouling context PDA emerges as a "double-edged sword". On the one hand it undoubtedly can serve as a universal "bioglue" applicable to a wide variety of materials, although the resulting surfaces have variable properties. Furthermore modification of the PDA with proteins, polymers and other molecules is readily achieved by reaction of the catechol/quinone groups in PDA with amino and thiol groups in the modifying macromolecule. By the same token, PDA can interact strongly with proteins (and possibly cells) in the contacting medium *via* reaction with their thiol and amino groups. Therefore unless masking of the PDA by PEG, BSA or other antifouling agent is 100% complete, some adsorption/adhesion will occur. It may be argued that the same consideration applies to any substrate, but the fact that protein–PDA interactions are so strong suggests a more serious problem.

Indeed in this work it is seen that on all three substrates PDA modification caused large increases in adsorption, by about 100% on PDMS and glass and 34% on PC. Thus attempts to confer protein resistance subsequently face a much greater challenge as reflected in the fact that treatment of the PDA surfaces with PEG gave surfaces with higher adsorption than the unmodified substrates in the case of PDMS and glass, and in the case of PC only a 40% decrease. Indeed, reductions in adsorption for the various modifications compared to the unmodified substrates, although significant, are not spectacular and are less than for other PEG modified surfaces.[47–50]

E. coli adhesion

Although extensive investigation of bacterial adhesion, as a measure of antifouling behaviour, was not carried out in the present work, a preliminary experiment was conducted on PDMS modified with PDA–PEG/BSA. The surface was first scratched with forceps to create a bare PDMS track prior to incubation in a suspension of *E. coli* transfected with GFP. As shown in Fig. 5, *E. coli* adhered preferentially to the bare PDMS area with much lower attachment on the PDA–PEG/BSA modified areas. This provides some evidence that this treatment may be useful for the inhibition of bacterial adhesion. However, the ease

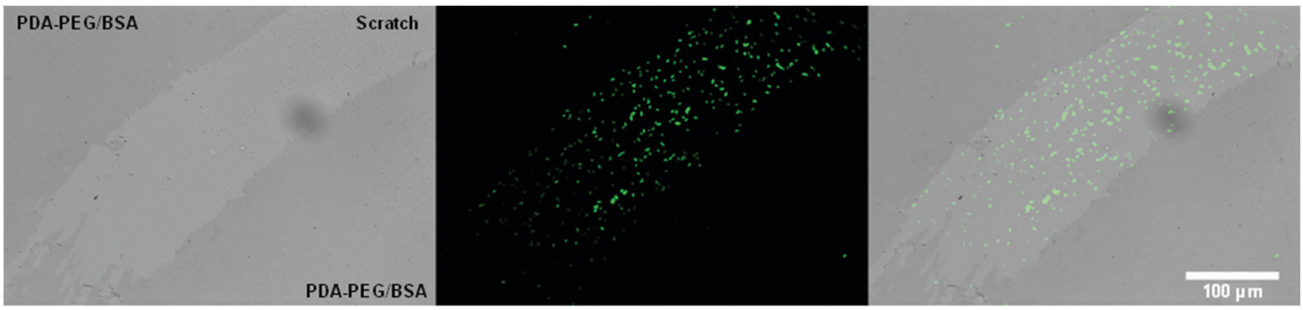

Fig. 5 Bright-field and fluorescence images of GFP transfected *E. coli* on a scratched PDMS–PDA–PEG/BSA surface. *E. coli* cells show preferential adhesion to scratched area and low cell adhesion on the adjacent PDA–PEG/BSA modified areas. 2×10^7 cells were seeded on PDMS for 4 h in PBS (pH 7.4).

of susceptibility to damage of the PDA coating emphasizes the need to prevent damage to PDA layers deposited on substrates.

Conclusion

PDA–PEG antifouling coatings on three substrate materials were investigated to evaluate the utility of PDA-based coatings for application to multiple materials. In addition the antifouling behaviour of PDA–PEG coatings backfilled with BSA was examined. Formation of PDA layers and the properties of the layers were strongly dependent on the wettability of the substrate: PDA interacted more strongly with the relatively hydrophobic PDMS than with the hydrophilic glass. Wettability differences resulted in differences in the PDA deposition mechanism on the three materials (polymerization of dopamine *vs.* adsorption of PDA particles), which in turn influenced the PDA thickness and surface roughness. Rougher PDA surfaces have greater true-to-nominal area ratio than smoother ones and thus can potentially have a higher graft density of PEG. This may explain the finding, based on contact angles, XPS data and resistance to fibrinogen adsorption, that the PEG density on the smoother PDMS–PDA was apparently relatively low compared to the other substrates. Although glass–PDA had high surface roughness, it also showed poor PEG grafting (based on resistance to fibrinogen adsorption), probably due to damage of the PDA layer and exposure of the substrate. PC–PDA with intermediate surface roughness showed the highest PEG density based on resistance to fibrinogen adsorption. It appears that PEG grafting on PDA layers is most efficient on surfaces with wettability similar to that of PDA (contact angle 50°–65°), thereby promoting wetting and polydopamine deposits of optimum roughness. Fibrinogen adsorption on the PDA surfaces was reduced upon attachment of PEG or BSA, but more for BSA attachment due to a greater density or more effective coverage of BSA compared to PEG. Backfilling PDA–BSA surfaces with PEG had no effect on fibrinogen adsorption again indicating that BSA coverage on these surfaces was high. Surfaces formed by backfilling the PDA–PEG surfaces with BSA showed still lower fibrinogen adsorption. PC surfaces, with presumably the greatest PEG density, showed the lowest adsorption among all the surfaces studied when backfilled with BSA.

From this work, PDA emerges as a "double-edged sword" with respect to the creation of antifouling surfaces. It has the ability to adhere to many types of substrate (albeit with variable properties of the deposited layers) and further modification with proteins and other biological molecules is readily achieved. However, proteins in any contacting medium will be readily adsorbed to PDA not covered. Backfilling of PDA–PEG with BSA virtually eliminated the effects of differences in PEG grafting on the three materials. Despite such disadvantages with the PDA approach, it may still be valid as a "universal" or substrate-independent method for conferring antifouling properties, and may therefore be useful as a simple method for modification of biomedical and biotechnological devices consisting of many materials.

Conflicts of interest

There are no conflicts to declare.

Acknowledgements

This work was supported in part by the Province of Ontario through an ORF-RE grant, the Natural Sciences and Engineering Council (NSERC) of Canada (QF and JB), and a Mitacs Globalink Award. QF held the Canada Research Chair in Biophotonics and SG was supported by the Ontario Graduate Scholarship (OGS). The authors acknowledge Deepinder Sharma for assisting in *E. coli* cell culture.

References

1 B. O'Flynn, F. Regan, A. Lawlor, J. Wallace, J. Torres and C. O'Mathuna, *Meas. Sci. Technol.*, 2010, **21**, 124004.
2 O. Korostynska, A. Mason and A. Al-Shamma'a, *Int. J. Smart Sens. Intell. Syst.*, 2012, **5**, 149–176.
3 L. Hsu, P. R. Selvaganapathy, J. L. Brash, Q. Fang, C.-Q. Xu, M. J. Deen and H. Chen, *IEEE Sens. J.*, 2014, **14**, 3400–3407.
4 K. M. Kovach, J. R. Capadona, A. S. Gupta and J. A. Potkay, *J. Biomed. Mater. Res., Part A*, 2014, **102**, 4195–4205.
5 H. Chen, L. Wang, Y. Zhang, D. Li, G. W. McClung, M. A. Brook, H. Sheardown and J. L. Brash, *Macromol. Biosci.*, 2008, **8**, 863–870.

6 J. M. Goddard and J. H. Hotchkiss, *Prog. Polym. Sci.*, 2007, **32**, 698–725.
7 A. Whelan and F. Regan, *J. Environ. Monit.*, 2006, **8**, 880–886.
8 S. Upadhyaya and R. P. Selvaganapathy, *Lab Chip*, 2010, **10**, 341–348.
9 M. Krishnamoorthy, S. Hakobyan, M. Ramstedt and J. E. Gautrot, *Chem. Rev.*, 2014, **114**, 10976–11026.
10 H. Lee, S. M. Dellatore, W. M. Miller and P. B. Messersmith, *Science*, 2007, **318**, 426–430.
11 W. J. Brittain and S. Minko, *J. Polym. Sci., Part A: Polym. Chem.*, 2007, **45**, 3505–3512.
12 E. Tziampazis, J. Kohn and P. V. Moghe, *Biomaterials*, 2000, **21**, 511–520.
13 O. Pop-Geogievski, S. Popelka, M. Houska, D. Chvostova, V. Proks and F. Rypacek, *Biomacromolecules*, 2011, **12**, 3232–3242.
14 R. Barbey, L. Lavanant, D. Paripovic, N. Schuwer, C. Sugnaux, S. Tugulu and H.-A. Klok, *Chem. Rev.*, 2009, **109**, 5437–5527.
15 D. R. Dreyer, D. J. Miller, B. D. Freeman, D. R. Paul and C. W. Bielawski, *Chem. Sci.*, 2013, **4**, 3796–3802.
16 S. H. Ku, J. Ryu, S. K. Hong, H. Lee and C. B. Park, *Biomaterials*, 2010, **31**, 2535–2541.
17 R. Zeng, Z. Luo, D. Zhou, F. Cao and Y. Wang, *Electrophoresis*, 2010, **31**, 3334–3341.
18 R. Wang, Y. Xie, T. Xiang, S. Sun and C. Zhao, *J. Mater. Chem. B*, 2017, **5**, 3035–3046.
19 J. Zhou, X. Guo, Q. Zheng, Y. Wu, F. Cui and B. Wu, *Colloids Surf., B*, 2017, **152**, 124–132.
20 H. Ye, Y. Xia, Z. Liu, R. Huang, R. Su, W. Qi, L. Wang and Z. He, *J. Mater. Chem. B*, 2016, **4**, 4084–4091.
21 L. Chen, R. Zeng, L. Xiang, Z. Luo and Y. Wang, *Anal. Methods*, 2012, **4**, 2852–2859.
22 H. W. Kim, H. D. Lee, S. J. Jang and H. B. Park, *J. Appl. Polym. Sci.*, 2015, 41661.
23 D. J. Miller, P. A. Araujo, P. B. Correia, M. M. Ramsey, J. C. Kruithof, M. C. van Loosdrecht, B. D. Freeman, D. R. Paul, M. Whiteley and J. S. Vrouwenvelder, *Water Res.*, 2012, **46**, 3737–3753.
24 W.-B. Tsai, C.-Y. Chien, H. Thissen and J.-Y. Lai, *Acta Biomater.*, 2011, **7**, 2518–2525.
25 H.-W. Chien and W.-B. Tsai, *Acta Biomater.*, 2012, **8**, 3678–3686.
26 T. S. Sileika, H.-D. Kim, P. Maniak and P. B. Messersmith, *ACS Appl. Mater. Interfaces*, 2011, **3**, 4602–4610.
27 L.-P. Zhu, J.-H. Jiang, B.-K. Zhu and Y.-Y. Xu, *Colloids Surf., B*, 2011, **86**, 111–118.
28 R. Huang, X. Liu, H. Ye, R. Su, W. Qi, L. Wang and Z. He, *Langmuir*, 2015, **31**, 12061–12070.
29 Y. Qian, Y. Zhang, H. Wang, J. L. Brash and H. Chen, *Acta Biomater.*, 2011, **7**, 1550–1557.
30 D. Zang, L. Ge, M. Yan, X. Song and J. Yu, *Chem. Commun.*, 2012, **48**, 4683–4685.
31 S. Cesaro-Tadic, G. Dernick, D. Juncker, G. Buurman, H. Kropshofer, B. Michel, C. Fattinger and E. Delamarche, *Lab Chip*, 2004, **4**, 563–569.
32 S. Hideshima, R. Sato, S. Inoue, S. Kuroiwa and T. Osaka, *Sens. Actuators, B*, 2012, **161**, 146–150.
33 S. A. Michel, M. L. Knetsch and L. H. Koole, *J. Biomater. Sci., Polym. Ed.*, 2014, **25**, 698–712.
34 H. Yamazoe and T. Tanabe, *J. Biomed. Mater. Res., Part A*, 2007, **86**, 228–234.
35 H. Yamazoe, T. Uemura and T. Tanabe, *Langmuir*, 2008, **24**, 8402–8404.
36 A. Revzin, P. Rajagopalan, A. W. Tilles, F. Berthiaume, M. L. Yarmush and M. Toner, *Langmuir*, 2004, **20**, 2999–3005.
37 E. Bulard, M.-P. Fontaine-Aupart, H. Dubost, W. Zheng, M.-N. Bellon-Fontaine, J.-M. Herry and B. Bourguignon, *Langmuir*, 2012, **28**, 17001–17010.
38 C. Nune, W. Xu and R. D. Misra, *J. Biomed. Mater. Res., Part A*, 2012, **100A**, 3197–3204.
39 C. F. Wertz and M. M. Santore, *Langmuir*, 2001, **17**, 3006–3016.
40 J. Jiang, L. Zhu, L. Zhu, B. Zhu and Y. Xu, *Langmuir*, 2011, **27**, 14180–14187.
41 S. Sharma, R. W. Johnson and T. A. Desai, *Biosens. Bioelectron.*, 2004, **20**, 227–239.
42 S. Nirasay, A. Badia, G. Leclair, J. P. Claverie and I. Marcotte, *Materials*, 2012, **5**, 2621–2636.
43 D. M. Doran and I. L. Spar, *J. Immunol. Methods*, 1980, **39**, 155–163.
44 H. Fujiwara, *Spectroscopic Ellipsometry: Principles and Applications*, John Wiley & Sons Ltd, Chichester, 2007.
45 R. Michel, S. Pasche, M. Textor and D. G. Castner, *Langmuir*, 2005, **21**, 12327–12332.
46 Q. Wei, F. Zhang, J. Li, B. Li and C. Zhao, *Polym. Chem.*, 2010, **1**, 1430–1433.
47 J. Tan and J. L. Brash, *J. Biomed. Mater. Res., Part A*, 2009, **90A**, 196–204.
48 S. Jo and K. Park, *Biomaterials*, 2000, **21**, 605–616.
49 S. Pasche, S. M. De Paul, J. Voros, N. D. Spencer and M. Textor, *Langmuir*, 2003, **19**, 9216–9225.
50 S. Pasche, J. Voros, H. J. Griesser, N. D. Spencer and M. Textor, *J. Phys. Chem. B*, 2005, **109**, 17545–17552.